Plant, Cell & Environment

WILEY

Plant, Cell & Environment

ORIGINAL ARTICLE

Single-Cell RNA-Sequencing of Soybean Reveals Transcriptional Changes and Antiviral Functions of GmGSTU23 and GmGSTU24 in Response to Soybean Mosaic Virus

Shuang Song[1,2] | Jing Wang[1] | Jiaying Zhou[2] | Xiaofei Cheng[2] | Yuxi Hu[1] | Jinhui Wang[1] | Jianan Zou[1] | Ying Zhao[1] | Chunyan Liu[1] | Zhenbang Hu[1] | Qingshan Chen[1] | Dawei Xin[1]

[1]National Key Laboratory of Smart Farm Technologies and Systems, College of Agriculture, Northeast Agricultural University, Harbin, China | [2]College of Plant Protection, Northeast Agricultural University, Harbin, China

Correspondence: Qingshan Chen (qschen@126.com) | Dawei Xin (dwxin@neau.edu.cn)

Received: 9 June 2024 | **Revised:** 20 August 2024 | **Accepted:** 6 September 2024

Funding: This work was supported by the National Natural Science Foundation of China (Grant numbers: 32301897, 32070274, 31771882, 32072014, U20A2027, 31801389, 32472149), the Lo Kwee Seong Foundation and Heilongjiang Provincial Key R&D Project (Grant number: JD2023GJ01-07).

Keywords: GST | single-cell RNA sequencing | SMV | soybean

ABSTRACT

Soybean mosaic virus (SMV) stands as a prominent and widespread threat to soybean (*Glycine max* L. Merr.), the foremost legume crop globally. Attaining a thorough comprehension of the alterations in the transcriptional network of soybeans in response to SMV infection is imperative for a profound insight into the mechanisms of viral pathogenicity and host resistance. In this investigation, we isolated 50 294 protoplasts from the newly developed leaves of soybean plants subjected to both SMV infection and mock inoculation. Subsequently, we utilized single-cell RNA sequencing (scRNA-seq) to construct the transcriptional landscape at a single-cell resolution. Nineteen distinct cell clusters were identified based on the transcriptomic profiles of scRNA-seq. The annotation of three cell types—epidermal cells, mesophyll cells, and vascular cells—was established based on the expression of orthologs to reported marker genes in *Arabidopsis thaliana*. The differentially expressed genes between the SMV- and mock-inoculated samples were analyzed for different cell types. Our investigation delved deeper into the tau class of glutathione S-transferases (GSTUs), known for their significant contributions to plant responses against abiotic and biotic stress. A total of 57 *GSTU* genes were identified by a thorough genome-wide investigation in the soybean genome *G. max* Wm82.a4.v1. Two specific candidates, *GmGSTU23* and *GmGSTU24*, exhibited distinct upregulation in all three cell types in response to SMV infection, prompting their selection for further research. The transient overexpression of GmGSTU23 or GmGSTU24 in *Nicotiana benthamiana* resulted in the inhibition of SMV infection, indicating the antiviral function of soybean GSTU proteins.

1 | Introduction

As obligate biotrophic pathogens, plant viruses rely on intricate molecular interactions between the cellular proteins of host plants and viral proteins to complete their life cycle within the host. Dissecting the molecular network of virus–plant interactions will not only benefit the understanding of virus pathogenesis but also advance the development of novel control

Shuang Song and Jing Wang contributed equally to this study.

strategies for plant viral disease (Wu and Cheng 2020). Many host factors have been identified as being involved in various steps of virus infection, such as viral protein translation, genome multiplication, intercellular movement and long-distance systemic transport (Wang 2015; Zhao et al. 2016; Wu and Cheng 2020). Virus–plant interactions are typically linked to substantial alterations in the expression of host factor genes (Havelda et al. 2008). Advancements in deep sequencing technology have led to the widespread use of high-throughput transcriptomics sequencing to investigate changes in gene expression induced by virus infection (Babu et al. 2008; Havelda et al. 2008). However, the traditional bulk RNA sequencing only reflects the average expression level of the diverse constituent cells in a sample and misses the heterogeneity in gene expression among cells. As a new and powerful technique, single-cell RNA sequencing (scRNA-seq) can characterize the precise gene expression patterns of thousands of individual cells from one sample (Potter 2018; Shaw, Tian, and Xu 2020). Although a growing number of applications of scRNA-seq in plants, especially in model plants like *Arabidopsis thaliana* (Kim et al. 2021; Lopez-Anido et al. 2021; Zhang, Chen, and Wang 2021; Procko et al. 2022) and rice (Wang et al. 2021), have been reported in recent years, the application of scRNA-seq in virus-infected plants remains absent.

Soybean (*Glycine max* L. Merr.) is the most important legume crop in the world. Among the various viruses infecting soybean, the soybean mosaic virus (SMV) stands out as the most prevalent and hazardous (Song et al. 2022). SMV infections on soybeans not only result in foliar symptoms such as mosaic, distortion and vein necrosis but also instigate seed coat mottling, leading to substantial production losses and compromising seed quality (Hajimorad et al. 2018; Zong et al. 2020; Song et al. 2022). SMV belongs to the genus *Potyvirus* within the family *Potyviridae* and possesses a positive-sense single-stranded RNA genome. The genome contains a large open reading frame (ORF) encoding a polyprotein and a small ORF that is expressed as a fusion protein named P3N-PIPO (pretty interesting *Potyviridae* ORF) by transcriptional slippage of the replicase at a GA_6 motif (Whitham et al. 2016). The polyprotein undergoes processing by SMV-encoded proteinases, leading to the production of 10 mature proteins, including protein 1 (P1), helper component protease (HC-Pro), protein 3 (P3), six-kilodalton 1 (6K1), cylindrical inclusion (CI), six-kilodalton 2 (6K2), virus genome-linked protein, nuclear inclusion a, nuclear inclusion b and coat protein (Whitham et al. 2016; Hajimorad et al. 2018).

Glutathione S-transferases (GSTs) are a family of enzymes that are widely present in cells of both eukaryotes and prokaryotes and catalyze the transfer of reduced glutathione (GSH; γ-Glu–Cys–Gly) to electrophilic centres of a wide variety of substrates (Chen et al. 2013; Skopelitou et al. 2015). Based on different criteria like sequence similarity, kinetic characteristics and immunological properties, the plant GSTs are classified into eight classes, including tau (U), phi (F), theta (T), zeta (Z), lambda (λ), dehydroascorbate reductase (DHAR), tetrachlorohydroquinone dehalogenase (TCHQD) and the γ-subunit of eukaryotic translation elongation factor 1B (EF1Bγ) (McGonigle et al. 2000; Ahmad et al. 2020). Of these classes, the tau GSTs (GSTUs) emerge as the most abundant in plants (Skopelitou et al. 2015). GSTUs in plants play important roles in responses to abiotic and biotic stress, including virus infection (McGonigle et al. 2000; Chen et al. 2013; Skopelitou et al. 2015).

In this work, we isolated protoplasts from newly developed systemic leaves of SMV-inoculated and mock-inoculated soybean plants and generated their transcriptional atlas at single-cell resolution. Three cell types, including epidermal cells, mesophyll cells and vascular cells, were determined from 19 cell clusters. A total of 57 *GmGST* genes of the tau class (*GmGSTUs*) were identified in the soybean genome (*G. max* Wm82.a4.v1), and their transcriptional changes in each type of cell between SMV-inoculated and mock-inoculated soybean plants were analyzed. Notably, *GmGSTU23* and *GmGSTU24* exhibited distinct upregulation in all three cell types in response to SMV infection and were subsequently confirmed to suppress viral infection.

2 | Materials and Methods

2.1 | Plant Growth and Inoculation

The SMV-susceptible soybean cultivar SN14 (Song et al. 2022) was cultivated in plastic pots (16 cm diameter, 18 cm height) within a growth chamber set at 23 ± 3°C with 70% relative humidity and a 16/8 h (day/night) photoperiod. As the viral source, an engineered full-length cDNA infectious clone of the SMV-SC7 strain (Gao et al. 2015), denoted as pSMV-GFP and harboring a GFP gene insertion between P1 and HC-Pro cistrons, was utilized. The pSMV-GFP vector was transformed into *Agrobacterium tumefaciens* strain GV3101 and subsequent infiltrated into *Nicotiana benthamiana* leaves following established procedures (Zaulda et al. 2022). The systemic leaves of inoculated *N. benthamiana* plants with GFP fluorescence at 10 days postinoculation (dpi) were collected and homogenized in 0.1 M sodium phosphate buffer (1:10 w/v) using a mortar and pestle as inoculum. Subsequently, 2-week-old soybean plants were mechanically inoculated by gently rubbing the inoculum on leaves with a paintbrush, followed by rinsing with tap water after 5 min. Systemically infected top young leaves were harvested for scRNA-seq when GFP fluorescence became evident at 7 dpi (Figure 1A). As negative controls, the top young leaves of soybean plants inoculated with sodium phosphate buffer were collected at the same time for scRNA-seq (Figure 1A).

2.2 | Protoplast Isolation

The harvested leaf samples were promptly cut into 4–5 mm strips using a scalpel blade. These strips were immediately immersed in an RNase-free enzyme solution (containing 1% (w/v) cellulase R10, 0.2% (w/v) macerozyme R10, 0.3% (w/v) pectinase Y23, 0.1% (w/v) bovine serum albumin [BSA], 0.4 M mannitol, 20 mM 2-(N-morpholino) ethanesulfonic acid, 20 mM KCl, and 10 mM $CaCl_2$, pH 5.7) in a small Petri dish. Subsequently, the strips underwent digestion in the dark at 28°C for 3 h with gentle shaking (30 rpm). The resulting protoplast suspension was then filtered using a 100 μm cell strainer to eliminate undigested tissue and debris, and subsequently centrifuged at room temperature at 200 g for 5 min. The resulting pellets were resuspended and washed twice with a

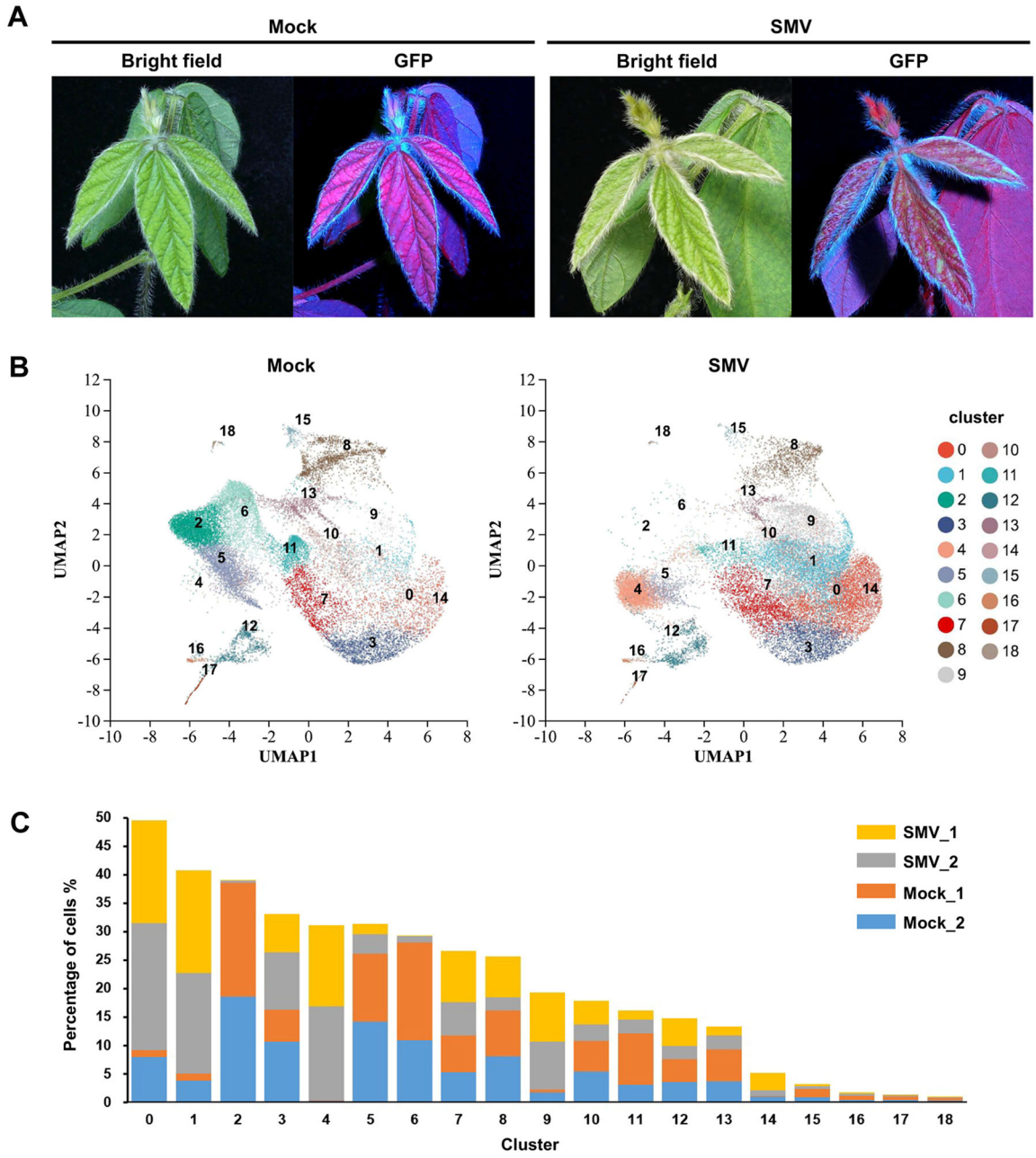

FIGURE 1 | Single-cell RNA-sequencing of the soybean leaves. (A) Top young leaves of systemically SMV-infected and mock-inoculated soybean plants were sampled for single-cell RNA-sequencing. (B) Uniform Manifold Approximation and Projection (UMAP) visualization of 19 distinct cell clusters from newly developed systemic leaves of SMV- and mock-inoculated soybean plants. Each dot represents a single cell and distinct cell clusters were marked by different colours. (C) Percentage of cells numbers allocated in the 19 cell clusters for two biological replicates of SMV- and mock-inoculated samples. [Color figure can be viewed at wileyonlinelibrary.com]

wash solution (containing 0.4 M mannitol and 0.1% (w/v) BSA, pH 5.7). Protoplast concentration and viability were assessed by staining with 0.04% (w/v) trypan blue and microscopic observation.

2.3 | scRNA Library Construction and Sequencing

Protoplast suspensions with a concentration ranging from 700 to 1200 cells/μL and a viability exceeding 80% underwent scRNA-seq at Shanghai Majorbio Bio-Pharm Technology Co., Ltd. (Shanghai, China). These suspensions were loaded into the 10× Genomics Chromium system to generate single-cell gel beads in emulsions (GEMs) and to construct scRNA-seq libraries using the Single Cell 3′ Library & Gel Bead Kit v.3 (10× Genomics, CA, USA) following the manufacturer's instructions. Subsequently, the libraries were sequenced on the Illumina NovaSeq. 6000 platform, producing 150 bp paired-end reads.

2.4 | scRNA-Seq Data Processing

Sequencing reads were processed through the Cell Ranger 4.0 pipeline from 10× Genomics, using default parameters.

Alignment to the reference genome *G. max* Wm82.a4.v1 was performed using the STAR algorithm (Le et al. 2017). Subsequently, gene-barcode matrices, encompassing barcoded cells and unique molecular identifier (UMI) counts, were generated. These matrices were then imported into the Seurat v3.2.0 R toolkit for subsequent analysis (Butler et al. 2018). The low-quality cells, including the ones with expressed genes below 500 and above 10 000, with UMIs below 500 and above 50 000, with the percentage of mitochondrial genes above 5%, and with the percentage of chloroplast genes above 10%, were filtered out for quality control (Zhang, Chen, and Wang 2021). Subsequently, the remaining data were normalized using the NormalizeData function in the Seurat package. Variable genes were determined using the FindVariableGenes function. Data integration from different samples was achieved through FindIntegrationAnchors and IntegrateData in the Seurat package. Principle component analysis was employed for dimensionality reduction, and distinctive cell clusters were visualized using Uniform Manifold Approximation and Projection (UMAP) with a 0.8 resolution based on the top 30 principal components (McInnes, Healy, and Melville 2018; Chen et al. 2019). Considering that no well-known marker genes for soybean leaf cells had been reported, expression profiles of the homologous genes of reported marker genes of *A. thaliana* for different cell clusters were analyzed to annotate each cluster. Average expression levels and percentages of cells expressing the marker genes per cluster were visualized in dot plots. The differentially expressed genes (DEGs) between different treatments, samples, cell types, or clusters were identified using the function FindMarkers in the Seurat package, with criteria of $|\log_2 FC| \geq 0.25$ and $p \leq 0.01$. The KEGG enrichment analyses of DEGs were performed on the Majorbio Cloud platform (https://cloud.majorbio.com/page/project/overview.html).

2.5 | RNA In Situ Hybridization

Fresh leaves were collected as described in scRNA-seq samples collection and fixed in FAA solution for 24 h at 4°C. The tissue blocks were cut into about 3 mm thick, dehydrated in graded alcohol, cleared in xylene and embedded in paraffin. The embedded samples were sliced into 6 μm sections, and the sections were treated with xylene, dehydrated with graded alcohol and digested with 200 μg/mL protease K. The digoxigenin-labelled probes were synthesized by GENWIZ (Suzhou, China) and their sequences were listed in Supporting Information S8: Table S6. The sections were incubated with probes overnight at 40°C. After washing, the sections were then incubated with alkaline phosphatase-conjugated anti-digoxin antibody at 40°C for 50 min, and detected by nitro-blue tetrazolium/5-bromo-4-chloro-3′-indolyphosphate solution. Photographs were taken using Nikon ECLIPSE-Ci.

2.6 | Identification and Analysis of *GST* Gene Family From Soybean Genome

Two GST N-terminal domains (Pfam 02798 and 13409) and two GST C-terminal domains (Pfam 00043 and 13410) were used as queries for BLASTp search of *GST* genes against the soybean genome database *G. max* Wm82.a4.v1 in Phytozome (https://phytozome-next.jgi.doe.gov/ blast-search). The MEME online tool (https://meme-suite.org/meme/) was used to identify conserved motifs in the deduced amino acid sequences (Bailey et al. 2009). Alignment of amino acid sequences was performed using the ClustalW algorithm in MEGA 11 (Tamura, Stecher, and Kumar 2021), and phylogenetic trees were constructed using the neighbour-joining method with 1000 bootstrap replicates. The alterations in expression levels of *GSTU* genes across different cell types in response to SMV inoculations were examined using normalized expression data. A heatmap illustrating these expression changes was generated using GraphPad Prism 8.0.

2.7 | *Agrobacterium*-Mediated Transient Expression of GSTUs in *N. benthamiana*

To generate the overexpression vectors pCB301-GmGSTU24 and pCB301-GmGSTU23, the full-length coding sequences of *GmGSTU24* and *GmGSTU23* were amplified by RT-PCR from soybean cultivar SN14 using primer pairs U24-F/U24-R and U23-F/U23-R (Supporting Information S9: Table S7), respectively, and cloned into the vector pCB301 under the control of the CaMV 35S promoter using the pEASY-Basic Seamless Cloning and Assembly Kit (TransGen Biotech, Beijing, China). The overexpression vectors were transformed into *A. tumefaciens* GV3101 via electrotransformation. The GV3101 isolates containing overexpression vectors and an SMV-GFP infection clone (pSMV-GFP) at an OD_{600} of 0.5 were mixed equally and infiltrated into *N. benthamiana* leaves as previously described (Song et al. 2022; Zaulda et al. 2022). GV3101 isolate containing an empty vector of pCB301 (pCB301-EV) was used as a control. The expression of GFP was monitored using a LUYOR-3410 handheld high-intensity UV lamp.

2.8 | qRT-PCR

Total RNA was extracted using TRIzol reagent (Invitrogen, Carlsbad, CA, USA), following the manufacturer's instructions. The first-strand cDNA was synthesized using the PrimeScript 1st Strand cDNA Synthesis Kit (TaKaRa, Dalian, China) and utilized for qPCR analyses. qPCR was conducted with specific primer pairs (Supporting Information S9: Table S7) using the ChamQ Universal SYBR qPCR Master Mix (Vazyme Biotech, Nanjing, China), according to the manufacturer's instructions. *NbEF1α* and *GmUKN1* served as the reference genes for *N. benthamiana* and soybean, respectively. The expression level was quantified using the $2^{-\Delta\Delta C_t}$ method.

3 | Results

3.1 | scRNA-Seq of Soybean Leaf Cells

To systematically study gene expression patterns and cellular heterogeneity of soybean leaf cells in response to SMV infection, the newly developed systemic leaves of soybean plants inoculated by the GFP-labelled SMV infection clone (SMV-GFP) were collected when the GFP fluorescence started to be observed at 7

dpi and used for the construction of a single-cell transcriptome atlas. The newly developed leaves of mock-inoculated soybean plants at the same growing stage were also collected as controls. Two replicates were included for both SMV-inoculated (S1 and S2) and mock-inoculated (C1 and C2) plants. Following enzymatic hydrolysis, the isolated protoplast cells underwent scRNA-seq utilizing the 10× Genomics Chromium and Illumina HiSeq platforms. A total of 485.22 GB of raw data was obtained from 50 294 cells (13 086 in S1, 13 579 in S2, 12 183 in C1 and 11 446 in C2), with an average of 31 946 reads and a median of 2551 genes per cell (Supporting Information S3: Table S1). For SMV-inoculated samples, 96.59% and 99.81% of cells were infected with SMV in S1 and S2, respectively. Using the transcriptomic profiles of cells from merged SMV-inoculated (S1 and S2) and mock-inoculated (C1 and C2) samples, 19 distinct cell clusters were identified through dimensionality reduction via the UMAP technique, visualized in two-dimensional space (Figure 1B). While the UMAP projections of SMV-inoculated and mock-inoculated samples exhibited similar topography, the proportions of cells in each cluster displayed a marked difference between the two conditions (Figure 1C). Clusters 0, 1, 4, 9 and 14 contained notably more cells, whereas clusters 2, 5, 6 and 18 contained fewer cells in SMV-inoculated samples than in mock-inoculated samples. These findings underscore that SMV infection induces substantial changes in the transcriptome of soybean systemic leaves.

3.2 | Functional Annotation of Soybean Leaf Cell Clusters

Given the absence of well-established marker genes for soybean leaf cells, the cell types of these clusters were annotated using homologous genes of reported marker genes in *A. thaliana* (Procko et al. 2022; Lopez-Anido et al. 2021; Kim et al. 2021). *Glyma.07G066800*, the homologue of the known guard cell marker gene *AT2G46070/MAP KINASE 12 (MPK12)* (Kim et al. 2021), was mostly expressed in clusters 0 and 3, and to a lesser extent, in clusters 1, 7 and 14. The homologues of *AT3G54420/EP3 CHITINASE (EP3)*, which is specifically expressed in hydathodes cells (Bürkle et al. 2003; Kim et al. 2021), *Glyma.11G124500* and *Glyma.13G346700*, were expressed in clusters 0, 1, 3, 9, and 14. In cluster 8, the homologues of the epiderma-specific *AT2G38540/LIPID TRANSFER PROTEIN 1 (LP1)* (Clark and Bohnert 1999), *Glyma.18G210900* and *Glyma.01G132500*, were specifically detected. Taken together, clusters 0, 1, 3, 7, 8, 9 and 14 were assigned as epidermal cells (Figure 2).

Several photosynthesis-related marker genes, including *CHLOROPHYLL A/B BINDING PROTEIN 3* (*CAB3*; *Glyma.08G082900* and *Glyma.05G128000*), *RUBISCO SMALL SUBUNIT 2B* (*RBCS2B*; *Glyma.13G046200*) and *LIGHT-HARVESTING COMPLEX I CHLOROPHYLL A/B BINDING PROTEIN 2* (*LHCA2*; *Glyma.07G047600*) (Procko et al. 2022; Zhang, Chen, and Wang 2021; Sawchuk et al. 2008), exhibited high specificity in clusters 2, 5, 6, 11, 13, 15 and 18. *Glyma.15G176900* which is the homologue of the known mesophyll cell marker *AT5G20630/GERMIN-LIKE PROTEIN SUBFAMILY 3 MEMBER 3* (*GER3*) (Zhang, Chen, and Wang 2021) and *Glyma.06G055500* which is the homologue of mesophyll cell marker *AT2G06520/PHOTOSYSTEM II SUBUNIT X* (*PSBX*) reported by Xia et al. (2022) were also highly expressed in these seven clusters. Therefore, clusters 2, 5, 6, 11, 13, 15 and 18 were assigned as mesophyll cells. In general, mesophyll cells are the largest cell population detected in leaf samples (Wang et al. 2021; Kim et al. 2021; Sun et al. 2023). In SMV-inoculated soybean leaf samples in this work, however, these seven clusters only made up 10.3% and 5.7% of the total cells from S1 and S2 samples, respectively. Considering the proximity of cluster 4 to mesophyll cells on the UMAP graph and its notably higher cell count in SMV-inoculated samples compared to mock-inoculated samples, we hypothesized that cluster 4 likely represents mesophyll cells, exhibiting significant changes in transcriptome in response to SMV infection. In summary, clusters 2, 4, 5, 6, 11, 13, 15 and 18 were designated as mesophyll cells (Figure 2).

In clusters 16 and 17, three genes, including *Glyma.08G163500*, *Glyma.01G106200* and *Glyma.19G211000*, which were the homologues of phloem cell markers *AT1G79430/ALTERED PHLOEM DEVELOPMENT* (*APL*), *AT3G03270/HYPOXIA RESPONSIVE UNIVERSAL STRESS PROTEIN 1* (*HRU1*), and *AT3G11930*, respectively (Procko et al. 2022; Bonke et al. 2003), and one gene, *Glyma.08G288100*, which was the homologue of xylem cell marker *AT5G19530/ACAULIS5* (*ACL5*) (Kim et al. 2021), were detected to be specifically expressed. Moreover, three phloem cell marker genes, including *FT-INTERACTING PROTEIN 1* (*FTIP1*; *Glyma.09G003400*), *SIEVE ELEMENT OCCLUSION-RELATED 1* (*SERO1*; *Glyma.08G130500*) and *CLAVATA3/ESR-RELATED 25* (*CLE25*; *Glyma.01G038900*) (Liu et al. 2012; Rüping et al. 2010; Zhang, Chen, and Wang 2021) were specifically expressed in cluster 17. Nevertheless, the homologue of the phloem cell marker gene *AT1G22710/SUCROSE TRANSPORTER 2* (*SUC2*; *Glyma.10G217900*) (Truernit and Sauer 1995) was exclusively expressed in cluster 16. Furthermore, *AT3G56240/COPPER CHAPERONE* (*CCH*), known to accumulate in sieve elements (Mira, Martínez-García, and Peñarrubia 2001; Xu et al. 2017), had its soybean homologue *Glyma.02G160500* specifically expressed in clusters 12, 16 and 17. Consequently, clusters 12, 16 and 17 were designated as vascular cells (Figure 2), although the discrimination between phloem and xylem cells could not be achieved in this study.

To verify the cell population definition, RNA in situ hybridization assays for three above-mentioned cell type-specific *Arabidopsis* ortholog marker genes in the soybean leaf were carried out. The results showed that *Glyma.13G346700*, *Glyma.15G176900* and *Glyma.08G163500* were highly expressed in epidermal, mesophyll and vascular cells, respectively (Supporting Information S1: Figure S1). Moreover, three cell type-specific genes identified in this work were also selected for RNA in situ hybridization assays to identify new marker genes. *Glyma.17g166600* that highly expressed in clusters 0, 1, 3 and 14 was more expressed in epidermal cells (Figure 3A), while *Glyma.15G057600* that highly expressed in clusters 2, 5, 6, 11, 13, 15 and 18 was more expressed in mesophyll cells (Figure 3B). A cluster 12 and 16-specifically expressed gene, *Glyma.10G039800*, exhibited specific expression in vascular cells (Figure 3C). These results supported the assignment of cell types and the availability of new cell marker genes in the soybean leaf.

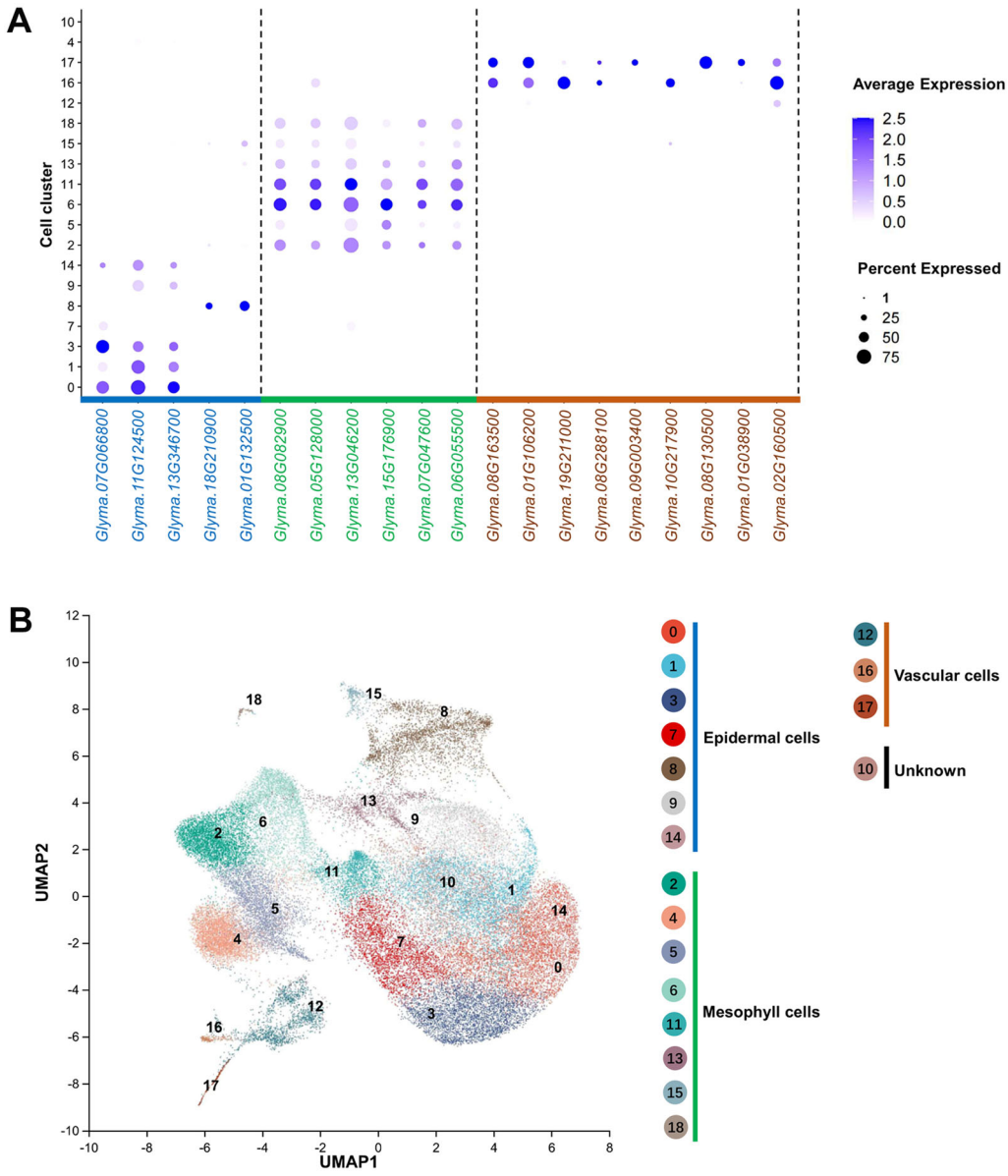

FIGURE 2 | Functional annotation of the 19 soybean leaf cell clusters. (A) Expression pattern of homologous genes orthologous to reported *Arabidopsis* leaf cell-type-specific marker genes used to assign cell types of the 19 clusters. The dot size represents the percentage of cells expressing the particular marker gene in the cluster, and dot colour intensity represents average expression level of marker genes. (B) Visualization of three leaf cell types including epidermal cells, mesophyll cells, vascular cells and an unknown type on the Approximation and Projection (UMAP) graph. [Color figure can be viewed at wileyonlinelibrary.com]

3.3 | SMV Infection Induced Transcriptomic Changes in Different Cell Types

The DEGs between the SMV- and mock-inoculated samples were detected with $|\log_2 FC| \geq 0.25$ and $p \leq 0.01$ for each cell type. As depicted in Figure 4A, a total of 2920 DEGs (1299 up, 1621 down), 2414 DEGs (971 up, 1443 down) and 3064 DEGs (1627 up, 1437 down) were detected in epidermal cells, mesophyll cells and vascular cells, respectively. Among these, 639 upregulated DEGs and 849 downregulated DEGs were common to all three cell types (Figure 4A). These 1488 DEGs in all three cell types were enriched in some pathways such as 'Photosynthesis', 'Ribosome', 'Photosynthesis – Antenna proteins', 'Glyoxylate, and dicarboxylate metabolism' and 'Carbon fixation in photosynthetic organisms' by KEGG pathway analysis (Figure 4B and Supporting Information S4: Table S2). In addition, there were also many DEGs that were only detected in a single cell type, including 674 (266 up, 408 down) in epidermal cells, 346 (113 up, 233 down) in mesophyll cells and 882 (491 up, 391 down) in vascular cells (Figure 4A). For cell type-specific DEGs in the epidermal cells, the five enriched KEGG pathways were 'Cyanoamino acid metabolism', 'Phenylpropanoid biosynthesis', 'Plant–pathogen interaction', 'Taurine and hypotaurine metabolism' and 'Carbon fixation in photosynthetic organisms' (Figure 4C and Supporting Information S5: Table S3). Only one KEGG pathway 'Photosynthesis' was enriched with $p < 0.05$ in mesophyll cell-specific DEGs (Figure 4D and Supporting Information S6: Table S4). The vascular cell-specific DEGs were enriched in three KEGG pathways, including 'Glutathione metabolism', 'Carbon fixation

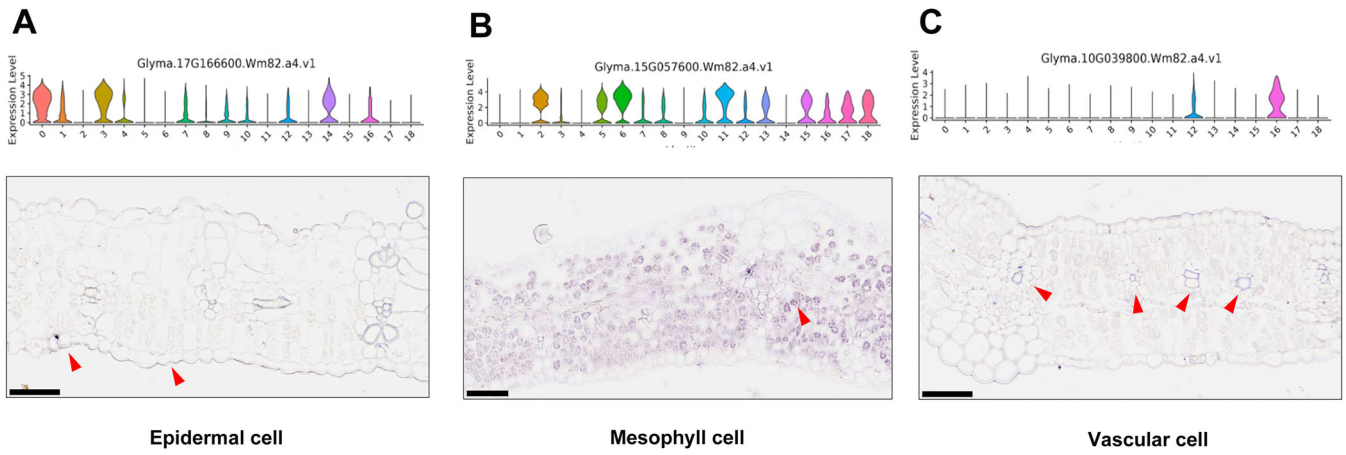

FIGURE 3 | Violin plots showing the expression patterns of new marker genes for soybean leaf cells and results of RNA in situ hybridization. (A) New marker gene for epidermal cells in the soybean leaf, *Glyma.17G166600.Wm82.a4.v1*. (B) New marker gene for mesophyll cells in the soybean leaf, *Glyma.15G057600.Wm82.a4.v1*. (C) New marker gene of vascular cells in the soybean leaf, *Glyma.10G039800.Wm82.a4.v1*. Scale bars represent 50 μm. [Color figure can be viewed at wileyonlinelibrary.com]

in photosynthetic organisms' and 'Ribosome' (Figure 4E and Supporting Information S7: Table S5).

3.4 | Genome-Wide Identification and Expression Patterns of *GST* Genes

GSTs are a group of enzymes with different roles in various physiology processes in plants and play an important role in stress tolerance. To analyze the function of GSTs in response to SMV infection in soybean, *GST* genes were identified by BLAST searches against the soybean genome database *G. max* Wm82.a4.v1 in Phytozome using two GST N-terminal domains (Pfam 02798 and 13409) and two GST C-terminal domains (Pfam 00043 and 13410) as queries. A total of 103 *GST* genes were identified in this genome-wide screen (Supporting Information S2: Figure S2). Phylogenetic analysis based on amino acid sequences using the neighbour-joining method divided them into 8 classes, including 57 *GST* genes in the U class, 12 genes in the F class, 10 genes in the TCHQD class, 9 in the λ class, 4 in each of the DHAR, EF1Bγ and T classes, and 3 in the Z class (Supporting Information S1: Figure S1). We retained the previous nomenclature scheme of *GSTU* genes by Ahmad et al. (2020), excluding *GmGSTU33* that was absent in the *G. max* Wm82.a4.v1 genome. The newly identified *GSTU* genes were designated from *GmGSTU38* to *GmGSTU58*, arranged based on their chromosomal positions from lowest to highest (Figure 5A). Subsequent analysis, utilizing the MEME online tool, uncovered eight conserved motifs. Among them, a previously identified GSTU-specific motif (VEEDLRNKSELLLKSNP VHKK) (Ahmad et al. 2020) was prevalent in most GSTU proteins, except for GmGSTU19, GmGSTU46 and GmGSTU53 (Figure 5B). Then, the expression patterns of *GSTU* genes in response to SMV infection were analyzed in different cell types (Figure 5C). Among the 57 *GSTU* genes, 9 (4 up and 5 down), 12 (7 up and 5 down) and 13 (12 up and 1 down) genes exhibited slight differential expression ($0.25 \leq |\log_2 FC| \leq 1$) in epidermal, mesophyll and vascular cells, respectively. Furthermore, 5 (3 up and 2 down), 5 (4 up and 1 down) and 7 (6 up and 1 down) genes displayed significant up- or downregulation ($|\log_2 FC| > 1$) in epidermal, mesophyll and vascular cells, respectively. Both *GmGSTU23* and *GmGSTU24* exhibited significant upregulation across all three cell types. *GmGSTU23* displayed the highest upregulation levels in mesophyll and vascular cells, boasting $\log_2 FC$ values of 3.046 and 3.025, respectively. *GmGSTU24* showcased the most substantial upregulation in epidermal cells with a $\log_2 FC$ value of 1.884. To further verify the scRNA-seq results, the expression patterns of *GmGSTU23* and *GmGSTU24* in the newly developed systemic leaves of SMV-inoculated soybean plants were detected by traditional qRT-PCR. It was showed that both *GmGSTU23* and *GmGSTU24* were upregulated in response to SMV infection from 5 dpi and reached the highest expression level at 7 dpi (Figure 5D). Taken together, *GmGSTU23* and *GmGSTU24* were chosen for further exploration of their gene functions.

3.5 | Transient Expression of GmGSTU24 or GmGSTU23 Inhibits SMV Infection in *N. benthamiana*

To investigate the role of GmGSTU24 and GmGSTU23 in SMV infection, *Agrobacterium*-mediated transient co-expression of each of GmGSTU24 (pCB301-GmGSTU24) and GmGSTU23 (pCB301-GmGSTU23) with the SMV-GFP infection clone (pSMV-GFP) at a ratio of 1:1 was performed in *N. benthamiana* leaves. A combination of empty vectors of pCB301 (pCB301-EV) and pSMV-GFP was inoculated as a control treatment. At 3 dpi, the fluorescence signal of GFP was observed in agroinfiltrated regions of control group plants only expressing SMV-GFP, and the fluorescence was stronger at 5 and 7 dpi (Figure 6A). However, only scattered fluorescence signals started to be observed at agroinfiltrated leaf vein regions that expressed GmGSTU24 and GmGSTU23 at 7 dpi (Figure 6A). The results of quantitative reverse transcription PCR (RT-qPCR) showed that the accumulation of viral genomic RNA was significantly lower in GmGSTU24- and GmGSTU23-expressing leaves than in the leaves of control plants at 5 and 7 dpi (Figure 6C). Despite the initiation of systemic SMV-GFP infection in all groups at 10 dpi, the fluorescence intensity was notably weaker in plants

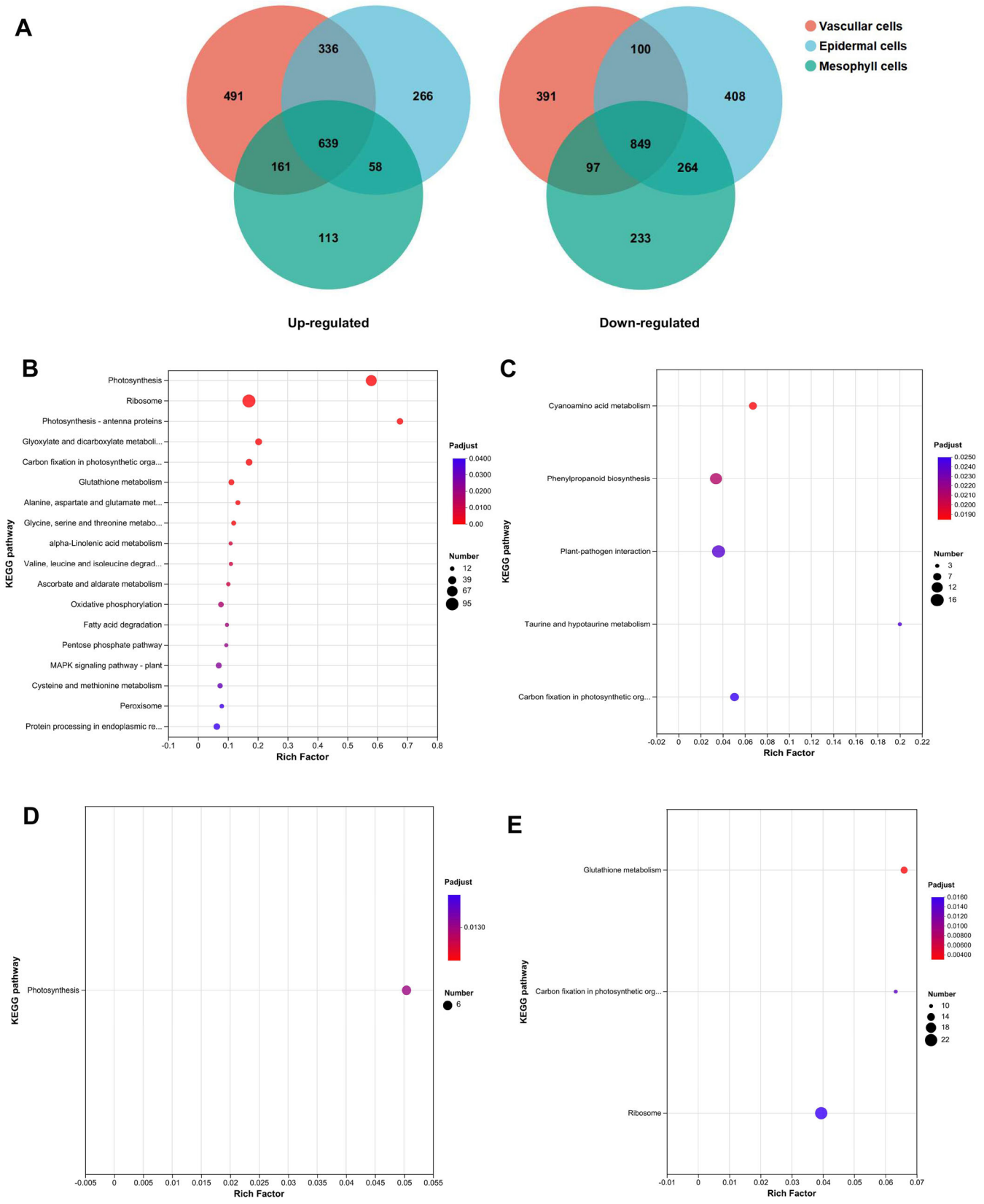

FIGURE 4 | Differentially expressed genes (DEGs) in response to SMV infection in different cell types. (A) Venn diagram of the number of up- and downregulated DEGs between different cell types. KEGG enrichment analysis of DEGs that in all of the three cell types (B), and that specific in epidermal cells (C), mesophyll cells (D) and vascular cells (E). [Color figure can be viewed at wileyonlinelibrary.com]

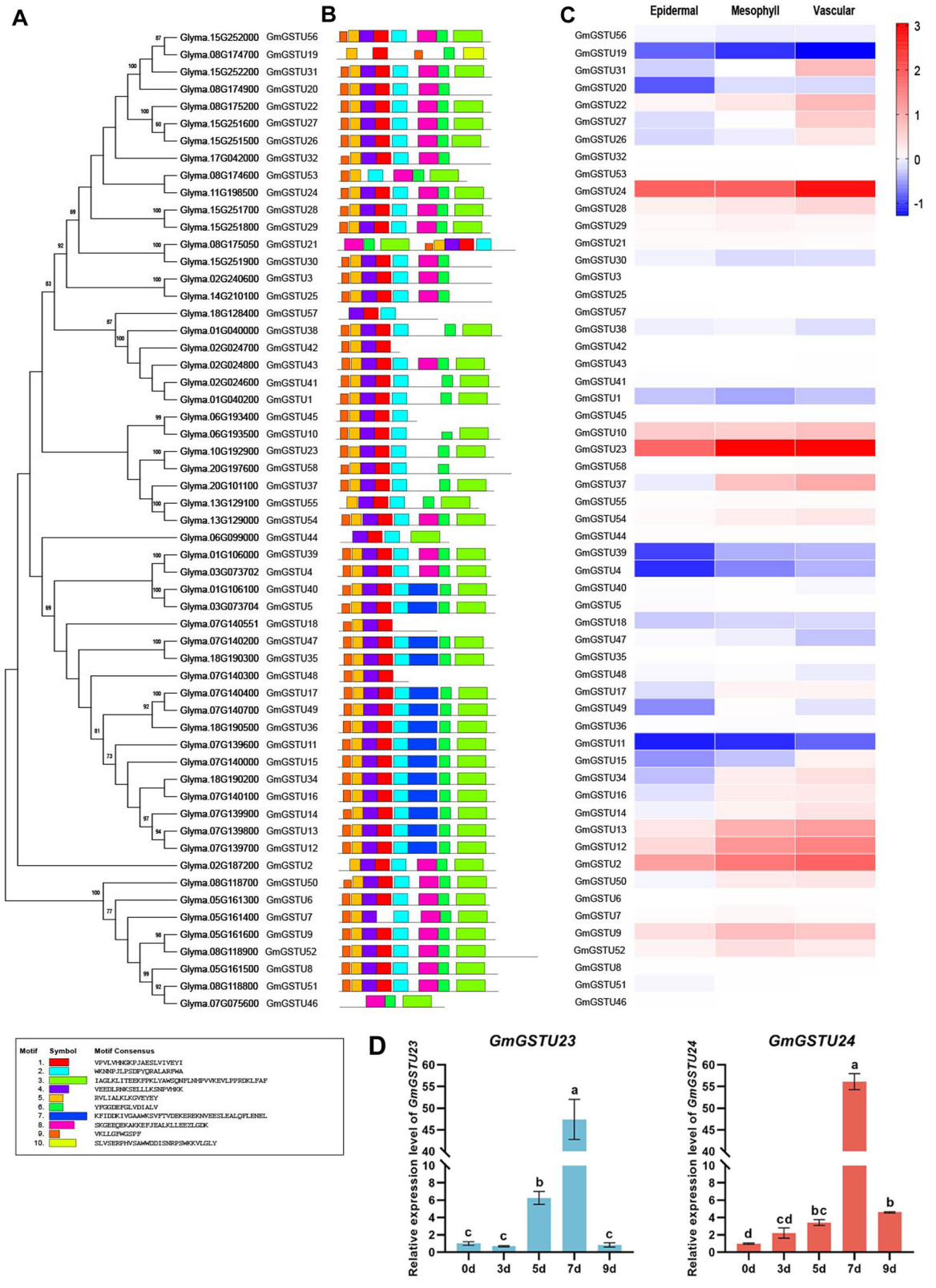

FIGURE 5 | Phylogenetic, motif analysis and cell type-specific expression of *GSTU* genes in soybean. (A) Phylogenetic neighbour-joining tree based on amino acid sequence of 57 *GSTU* genes constructed by MEGA11 with 1000 bootstrap replicates. (B) Schematic organization of conserved motifs in GmGSTU proteins. Different motifs are indicated by different colour blocks. (C) Expression profiles of *GmGSTU* genes in different cell types. The relative transcript abundance of genes are indicated by colour key. (D) Traditional qRT-PCR analysis of expression patterns of *GmGSTU23* and *GmGSTU24* in top young leaves of SMV-inoculated soybean plants at 0, 3, 5, 7 and 9 days postinoculation. [Color figure can be viewed at wileyonlinelibrary.com]

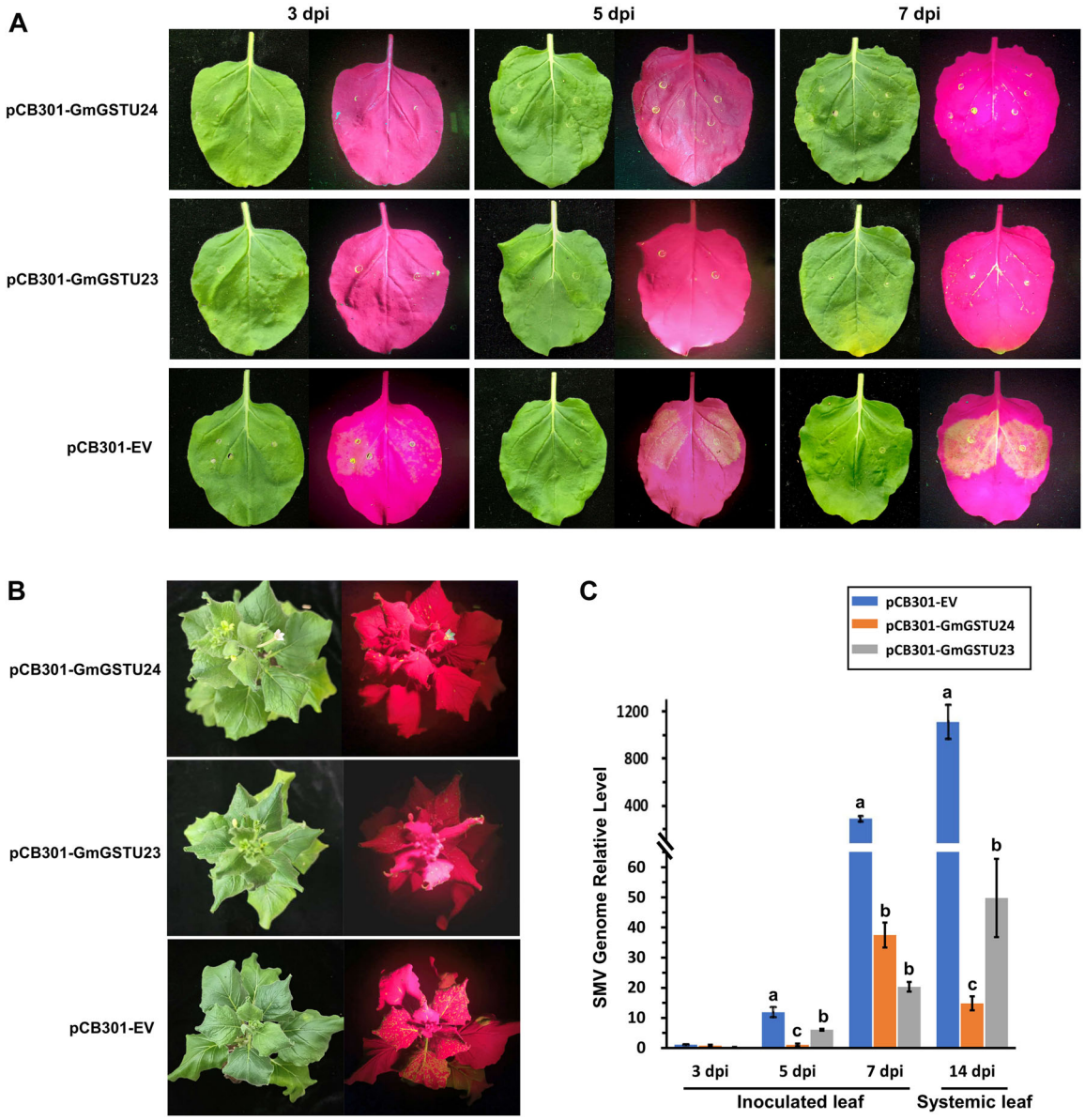

FIGURE 6 | Effect of GmGSTU24 and GmGSTU23 on SMV infection in *Nicotiana benthamiana*. The SMV-GFP infection clone was transiently co-expressed with each of pCB301-GmGSTU24, pCB301-GmGSTU23 and the empty vector pCBb301-EV as control. SMV-driven GFP expression on (A) inoculated leaves at 3, 5 and 7 days postinoculation (dpi) and (B) systemic leaves at 14 dpi were photographed under UV light. (C) qRT-PCR analysis showing relative level of SMV genomic RNA in inoculated leaves at 3, 5, 7 dpi and systemic leaves at 14 dpi. Different lowercase letters indicate significant differences at each timepoint with $p < 0.01$. [Color figure can be viewed at wileyonlinelibrary.com]

expressing GmGSTU24 and GmGSTU23 than in the control group (Figure 6B). These findings suggest that GmGSTU24 and GmGSTU23 exhibit antiviral properties against SMV infection.

4 | Discussion

Traditional bulk RNA sequencing is constrained by technical limitations, restricting the analysis to pooled cell populations of tissues, organs or entire organisms. Consequently, it fails to capture the heterogeneity in gene expression among individual cells (Potter 2018; Shaw, Tian, and Xu 2020). Recent advancements in scRNA-seq technologies have successfully addressed this limitation, allowing for gene expression analysis at the resolution of individual cells. Recently, researchers have applied this technology to analyze the single-cell transcriptome of cell subsets infected with human viruses such as Zika virus (Nowakowski et al. 2016; Onorati et al. 2016), human immunodeficiency virus (Rato et al. 2017) and cytomegalovirus (Johnson et al. 2017). This approach aims to explore specific features pertinent to virus–host interactions (Cristinelli and Ciuffi 2018). In the realm of plant research, the majority of the limited studies utilizing scRNA-seq have been conducted on model plants such as *A. thaliana*. These studies primarily concentrate on the identification of cell types and the construction of developmental trajectories (Shaw, Tian, and Xu 2020; Kim et al. 2021; Zhang, Chen, and Wang 2021). Some research about the single-cell transcriptome of plants in response to abiotic stresses has also been reported, for example, the single-cell transcriptome atlas of Chinese cabbage leaf

under heat stress (Sun et al. 2022) and those of rice in response to low-nitrogen, high-salinity and iron-deficient conditions (Wang et al. 2021). This study profiled the single-cell transcriptomes of cells from systemic young leaves of SMV-inoculated and mock-inoculated soybean plants. Over 50 000 individual cells were collected and categorized into 19 clusters based on their transcriptome features. Subsequently, three distinct cell types were delineated. To the best of our knowledge, this marks the inaugural instance of a single-cell transcriptome analysis detailing a plant's response to viral infection.

In this work, thousands of DEGs between the SMV- and mock-inoculated samples were detected for each cell type. The leaf epidermis is the first barrier to pathogen defence. Therefore, some epidermal cell-specific DEGs were enriched in the pathways of plant–pathogen interaction. Photosynthesis is a critical and fundamental life process for plants, and mesophyll cells of leaves are the principal centres of photosynthesis. We found that not only the DEGs in all three cell types but also those specific in mesophyll cells were enriched in photosynthesis-related pathways. It was indicated that photosynthesis process could be affected in the early stage of virus infection and SMV may inhibit soybean growth by reducing the efficiency of photosynthesis. Plant vascular tissues are not only the transport channels of water, sugar, hormones and other small signalling molecules, but also the channels of long-distance movement of viruses in plants. In this work, the largest amount of DEGs were identified from vascular cells, although the relative proportion of vascular cells number was the least. The KEGG analyses enriched the vascular cell-specific DEGs into three pathways with $p < 0.05$, and among them, the pathway of 'Glutathione metabolism' showed the highest significance with a p value of 3.9×10^{-3} (Supporting Information S7: Table S5). GSTs play important roles in GSH metabolism in plants. Therefore, we chose *GST* genes for further studies of gene expression and function.

The *GST* gene family, encompassing a substantial number of members in plants, can be categorized into distinct classes (Skopelitou et al. 2015). In soybean, McGonigle et al. (2000) identified 25 *GST* genes from an extensive expressed sequence tag database, classifying them into three types: I, II and III. Ahmad et al. (2020) expanded this repertoire, identifying 74 *GST* genes in the soybean genome through a BLASTp search in the Phytozome 12.1 database. They further classified them into eight classes, with the U class being the largest, incorporating 37 *GST* genes. In this study, a comprehensive genome-wide exploration of the soybean genome *G. max* Wm82.a4.v1 unveiled 103 *GST* genes, including 57 *GSTU* genes. Notably, 21 GSTs in the U class, 7 in the TCHQD class, 4 in the λ class and 2 in the F class were newly identified.

Plant GSTs exhibit a diverse array of functions. Initially identified in 1970, they were linked to the detoxification of herbicide injuries (Frear and Swanson 1970). It has been documented that the transcriptional levels of *GST* genes can be induced by various environmental stimuli (Marrs 1996; McGonigle et al. 2000). For instance, upon infection by *Colletotrichum orbiculare*, the expression levels of *NbGSTU1* and *NbGSTU3* in *N. benthamiana* were upregulated, while those of *NbGSTU2* remained unaffected (Dean, Goodwin, and Hsiang 2005). Skopelitou et al. (2015) found that *GmGSTU10* in soybean leaf tissues was specifically expressed in response to SMV infection. These findings suggested that maybe only a few GSTs among the large GST gene family are involved in disease development (Dean, Goodwin, and Hsiang 2005; Chen et al. 2013). Therefore, we analyzed the expression patterns of all the 57 *GSTU* genes in epidermal, mesophyll and vascular cells in response to SMV infection and found that three *GSTU* genes (*GmGSTU2*, *GmGSTU23* and *GmGSTU24*) were significantly upregulated in all of three cell types. Subsequent investigations revealed that the transient expression of GmGSTU23 or GmGSTU24 could impede the accumulation of SMV in *N. benthamiana*. In a study by Chen et al. (2013), *NbGSTU4* was identified as an upregulated gene following bamboo mosaic virus (BaMV) infection in *N. benthamiana*. Interestingly, NbGSTU4 was found to interact with the 3′ untranslated region (UTR) of BaMV genomic RNA, facilitating viral RNA accumulation (Chen et al. 2013). These findings imply that GSTs in distinct virus–host systems may assume diverse roles in disease development.

Acknowledgements

This work was supported by the National Natural Science Foundation of China (Grant numbers: 32301897, 32070274, 31771882, 32072014, U20A2027, 31801389, 32472149), the Lo Kwee Seong Foundation and Heilongjiang Provincial Key R&D Project (Grant number: JD2023GJ01-07).

Conflicts of Interest

The authors declare no conflicts of interest.

Data Availability Statement

The data that support the findings of this study are available from the corresponding author upon reasonable request.

References

Ahmad, M. Z., J. A. Nasir, S. Ahmed, et al. 2020. "Genome-Wide Analysis of Glutathione S-Transferase Gene Family in *G. max*." *Biologia* 75: 1691–1705.

Babu, M., A. G. Gagarinova, J. E. Brandle, and A. Wang. 2008. "Association of the Transcriptional Response of Soybean Plants With Soybean Mosaic Virus Systemic Infection." *Journal of General Virology* 89: 1069–1080.

Bailey, T. L., M. Boden, F. A. Buske, et al. 2009. "MEME Suite: Tools for Motif Discovery and Searching." *Nucleic Acids Research* 37: W202–W208.

Bonke, M., S. Thitamadee, A. P. Mähönen, M. T. Hauser, and Y. Helariutta. 2003. "APL Regulates Vascular Tissue Identity in *Arabidopsis*." *Nature* 426: 181–186.

Bürkle, L., A. Cedzich, C. Döpke, et al. 2003. "Transport of Cytokinins Mediated by Purine Transporters of the PUP Family Expressed in Phloem, Hydathodes, and Pollen of *Arabidopsis*." *Plant Journal* 34: 13–26.

Butler, A., P. Hoffman, P. Smibert, E. Papalexi, and R. Satija. 2018. "Integrating Single-Cell Transcriptomic Data Across Different Conditions, Technologies, and Species." *Nature Biotechnology* 36: 411–420.

Chen, I. H., M. H. Chiu, S. F. Cheng, Y. H. Hsu, and C. H. Tsai. 2013. "The Glutathione Transferase of *Nicotiana benthamiana* NbGSTU4 Plays a Role in Regulating the Early Replication of *Bamboo Mosaic Virus*." *New Phytologist* 199: 749–757.

Chen, Y., K. Li, X. Chu, L. B. Carey, and W. Qian. 2019. "Synchronized Replication of Genes Encoding the Same Protein Complex in Fast-Proliferating Cells." *Genome Research* 29: 1929–1938.

Clark, A. M., and H. J. Bohnert. 1999. "Cell-Specific Expression of Genes of the Lipid Transfer Protein Family From *Arabidopsis thaliana*." *Plant and Cell Physiology* 40: 69–76.

Cristinelli, S., and A. Ciuffi. 2018. "The Use of Single-Cell RNA-Seq to Understand Virus-Host Interactions." *Current Opinion in Virology* 29: 39–50.

Dean, J. D., P. H. Goodwin, and T. Hsiang. 2005. "Induction of Glutathione S-Transferase Genes of *Nicotiana benthamiana* Following Infection by *Colletotrichum destructivum* and *C. orbiculare* and Involvement of One in Resistance." *Journal of Experimental Botany* 56: 1525–1533.

Frear, D. S., and H. R. Swanson. 1970. "Biosynthesis of s-(4-Ethylamino-6-Isopropylamino-2-s-Triazino) Glutathione: Partial Purification and Properties of a Glutathione S-Transferase From Corn." *Phytochemistry* 9: 2123–2132.

Gao, L., R. Zhai, Y. K. Zhong, et al. 2015. "Screening Isolates of Soybean Mosaic Virus for Infectivity in a Model Plant, *Nicotiana benthamiana*." *Plant Disease* 99: 442–446.

Hajimorad, M. R., L. L. Domier, S. A. Tolin, S. A. Whitham, and M. A. Saghai Maroof. 2018. "Soybean Mosaic Virus: A Successful Potyvirus With a Wide Distribution but Restricted Natural Host Range." *Molecular Plant Pathology* 19: 1563–1579.

Havelda, Z., É. Várallyay, A. Válóczi, and J. Burgyán. 2008. "Plant Virus Infection-Induced Persistent Host Gene Downregulation in Systemically Infected Leaves." *Plant Journal* 55: 278–288.

Johnson, T. S., Z. B. Abrams, X. Mo, Y. Zhang, and K. Huang. 2017. "Lack of Human Cytomegalovirus Expression in Single Cells From Glioblastoma Tumors and Cell Lines." *Journal of NeuroVirology* 23: 671–678.

Kim, J. Y., E. Symeonidi, T. Y. Pang, et al. 2021. "Distinct Identities of Leaf Phloem Cells Revealed by Single Cell Transcriptomics." *Plant Cell* 33: 511–530.

Le, D. T., J. N. Durham, K. N. Smith, et al. 2017. "Mismatch Repair Deficiency Predicts Response of Solid Tumors to PD-1 Blockade." *Science* 357: 409–413.

Liu, L., C. Liu, X. Hou, et al. 2012. "FTIP1 Is an Essential Regulator Required for Florigen Transport." *PLoS Biology* 10: e1001314.

Lopez-Anido, C. B., A. Vatén, N. K. Smoot, et al. 2021. "Single-Cell Resolution of Lineage Trajectories in the *Arabidopsis* Stomatal Lineage and Developing Leaf." *Developmental Cell* 56: 1043–1055.e4.

Marrs, K. A. 1996. "The Functions and Regulation of Glutathione S-Transferases in Plants." *Annual Review of Plant Physiology and Plant Molecular Biology* 47: 127–158.

McGonigle, B., S. J. Keeler, S. M. C. Lau, M. K. Koeppe, and D. P. O'Keefe. 2000. "A Genomics Approach to the Comprehensive Analysis of the Glutathione S-Transferase Gene Family in Soybean and Maize." *Plant Physiology* 124: 1105–1120.

McInnes, L., J. Healy, and J. Melville. 2018. "UMAP: Uniform Manifold Approximation and Projection for Dimension Reduction." *arXiv*: 180203426.

Mira, H., F. Martínez-García, and L. Peñarrubia. 2001. "Evidence for the Plant-Specific Intercellular Transport of the *Arabidopsis* Copper Chaperone CCH." *Plant Journal* 25: 521–528.

Nowakowski, T. J., A. A. Pollen, E. Di Lullo, C. Sandoval-Espinosa, M. Bershteyn, and A. R. Kriegstein. 2016. "Expression Analysis Highlights AXL as a Candidate Zika Virus Entry Receptor in Neural Stem Cells." *Cell Stem Cell* 18: 591–596.

Onorati, M., Z. Li, F. Liu, et al. 2016. "Zika Virus Disrupts Phospho-TBK1 Localization and Mitosis in Human Neuroepithelial Stem Cells and Radial Glia." *Cell Reports* 16: 2576–2592.

Potter, S. S. 2018. "Single-Cell RNA Sequencing for the Study of Development, Physiology and Disease." *Nature Reviews Nephrology* 14: 479–492.

Procko, C., T. Lee, A. Borsuk, et al. 2022. "Leaf Cell-Specific and Single-Cell Transcriptional Profiling Reveals a Role for the Palisade Layer in UV Light Protection." *Plant Cell* 34: 3261–3279.

Rato, S., A. Rausell, M. Muñoz, A. Telenti, and A. Ciuffi. 2017. "Single-Cell Analysis Identifies Cellular Markers of the HIV Permissive Cell." *PLoS Pathogens* 13: e1006678.

Rüping, B., A. M. Ernst, S. B. Jekat, et al. 2010. "Molecular and Phylogenetic Characterization of the Sieve Element Occlusion Gene Family in Fabaceae and Non-Fabaceae Plants." *BMC Plant Biology* 10: 219.

Sawchuk, M. G., T. J. Donner, P. Head, and E. Scarpella. 2008. "Unique and Overlapping Expression Patterns Among Members of Photosynthesis-Associated Nuclear Gene Families in *Arabidopsis*." *Plant Physiology* 148: 1908–1924.

Shaw, R., X. Tian, and J. Xu. 2020. "Single-Cell Transcriptome Analysis in Plants: Advances and Challenges." *Molecular Plant* 14: 115–126.

Skopelitou, K., A. W. Muleta, A. C. Papageorgiou, E. Chronopoulou, and N. E. Labrou. 2015. "Catalytic Features and Crystal Structure of a Tau Class Glutathione Transferase From *Glycine max* Specifically Up-regulated in Response to Soybean Mosaic Virus Infection." *Biochimica et Biophysica Acta (BBA) – Proteins and Proteomics* 1854: 166–177.

Song, S., J. Wang, X. Yang, et al. 2022. "*GsRSS3L*, a Candidate Gene Underlying Soybean Resistance to Seedcoat Mottling Derived From Wild Soybean (*Glycine soja* Sieb. and Zucc.)." *International Journal of Molecular Sciences* 23: 7577.

Sun, X., D. Feng, M. Liu, et al. 2022. "Single-Cell Transcriptome Reveals Dominant Subgenome Expression and Transcriptional Response to Heat Stress in Chinese Cabbage." *Genome Biology* 23: 262.

Sun, Y., Y. Han, K. Sheng, et al. 2023. "Single-Cell Transcriptomic Analysis Reveals the Developmental Trajectory and Transcriptional Regulatory Networks of Pigment Glands in *Gossypium bickii*." *Molecular Plant* 16: 694–708.

Tamura, K., G. Stecher, and S. Kumar. 2021. "MEGA11: Molecular Evolutionary Genetics Analysis Version 11." *Molecular Biology and Evolution* 38: 3022–3027.

Truernit, E., and N. Sauer. 1995. "The Promoter of the *Arabidopsis thaliana* SUC2 Sucrose-H+ Symporter Gene Directs Expression of β-Glucuronidase to the Phloem: Evidence for Phloem Loading and Unloading by SUC2." *Planta* 196: 564–570.

Wang, A. 2015. "Dissecting the Molecular Network of Virus-Plant Interactions: The Complex Roles of Host Factors." *Annual Review of Phytopathology* 53: 45–66.

Wang, Y., Q. Huan, K. Li, and W. Qian. 2021. "Single-Cell Transcriptome Atlas of the Leaf and Root of Rice Seedlings." *Journal of Genetics and Genomics* 48: 881–898.

Whitham, S. A., M. Qi, R. W. Innes, W. Ma, V. Lopes-Caitar, and T. Hewezi. 2016. "Molecular Soybean-Pathogen Interactions." *Annual Review of Phytopathology* 54: 443–468.

Wu, X., and X. Cheng. 2020. "Intercellular Movement of Plant RNA Viruses: Targeting Replication Complexes to the Plasmodesma for Both Accuracy and Efficiency." *Traffic* 21: 725–736.

Xia, K., H. X. Sun, J. Li, et al. 2022. "The Single-Cell Stereo-Seq Reveals Region-Specific Cell Subtypes and Transcriptome Profiling in *Arabidopsis* Leaves." *Developmental Cell* 57: 1299–1310.e4.

Xu, Z., L. Gao, M. Tang, et al. 2017. "Genome-Wide Identification and Expression Profile Analysis of *CCH* Gene Family in *Populus*." *Peer J* 5: e3962.

Zaulda, F. A., S. H. Yang, J. Han, S. Mlotshwa, A. Dorrance, and F. Qu. 2022. "A Cowpea Severe Mosaic Virus-Based Vector Simplifies Virus-

Induced Gene Silencing and Foreign Protein Expression in Soybean." *Plant Methods* 18: 116.

Zhang, T. Q., Y. Chen, and J. W. Wang. 2021. "A Single-Cell Analysis of the *Arabidopsis* Vegetative Shoot Apex." *Developmental Cell* 56: 1056–1074.e8.

Zhao, J., X. Zhang, Y. Hong, and Y. Liu. 2016. "Chloroplast in Plant-Virus Interaction." *Frontiers in Microbiology* 7: 1565.

Zong, T., J. Yin, T. Jin, et al. 2020. "A DnaJ Protein That Interacts With Soybean Mosaic Virus Coat Protein Serves as a Key Susceptibility Factor for Viral Infection." *Virus Research* 281: 197870.

Supporting Information

Additional supporting information can be found online in the Supporting Information section.